

MALIN 1: A QUIESCENT DISK GALAXY^{1,2}

CHRIS IMPEY

Steward Observatory, University of Arizona

AND

GREG BOTHUN

Astronomy Department, University of Michigan

Received 1988 June 23; accepted 1988 October 27

ABSTRACT

We present new optical and radio spectroscopic observations of the remarkable galaxy Malin 1. This galaxy has unique features that include an extremely low surface brightness disk with an enormous mass of neutral hydrogen, and a low-luminosity Seyfert nucleus. Malin 1 is exceptional in its values of M_{HI} , L_B , and M_{HI}/L_B , and modest in its surface mass density of gas and stars. Spirals with large M_{HI}/L_B tend to have low mean column densities of H I and are close to the threshold for star formation caused by instabilities in a rotating gas disk. In these terms, Malin 1 has a disk with extremely inefficient star formation. The bulge spectrum is dominated by the absorption features of an old, metal-rich stellar population, although there is some evidence for hot (young) stars. The emission line excitations and widths in the nucleus are typical of a Seyfert galaxy; but Malin 1 is in the lowest 5% of the luminosity function of Seyferts, despite a copious fuel supply. Malin 1 is in a low-density region of the universe. We propose it as an unevolving disk galaxy, where the surface mass density is so low that the chemical composition and mass fraction in gas change very slowly over a Hubble time. Its properties are similar to those of the damped Ly α absorption systems seen in the spectra of high-redshift quasars. We emphasize that there are strong observational selection effects against finding gas-rich galaxies that are both massive and diffuse. Finally, we suggest that large and massive H I disks may have formed as early as $z \sim 2$, and remained quiescent to the present day.

Subject headings: galaxies: individual (Malin 1) — galaxies: photometry — galaxies: Seyfert — galaxies: stellar content — radio sources: 21 cm radiation — stars: formation

I. INTRODUCTION

Galaxy formation is one of the most fundamental and mysterious processes in cosmology. Considerable observational effort has been devoted to finding stellar systems that are young, gas-rich, and possibly in the act of collapsing. Indicators of a young galaxy can include a lack of old stars, prodigious star formation, a large ratio of gas to stars, and primordial chemical composition. Recent attention has focused on galaxies that are forming stars at high redshift. Stellar systems with high star formation rates have been found at redshifts up to 3.4 (Lilly 1988; McCarthy *et al.* 1987; Spinrad *et al.* 1985). However, most of these galaxies are found by their association with luminous radio sources, and since only one in 10^9 galaxies create nonthermal activity of such intensity, these systems may not shed light on galaxy formation in general (but see also the population of galaxies found recently by Cowie *et al.* 1988). Young galaxies have been indirectly detected by their absorption in quasar spectra. Wolfe *et al.* (1986) have argued that the damped Ly α systems seen at $z \sim 2$ in the spectra of many quasars are the progenitors of present day disk galaxies. Young galaxies may also be found at low redshift. Recently, Bergvall and Jörsäter (1988) have discovered a blue compact dwarf galaxy with an enormous star formation rate and a massive H I halo. However, it is often forgotten that

disk galaxy formation can be an unspectacular process that continues to the present day. There are strong technological limitations against finding galaxies with large fractions of their mass in neutral gas. If these galaxies are in addition large and diffuse, then the evolution and star formation rate can be extremely slow. In this paper we argue that Malin 1 is an example of such a quiescent or nonevolving galaxy.

Malin 1 is a galaxy at a redshift of $z = 0.083$ which is distinguished by an enormous, H I-rich, low surface brightness disk. Its discovery was reported by Bothun *et al.* (1987, hereafter BIMM) as part of a survey of low surface brightness galaxies in the Virgo cluster. First results of the survey have been presented by Impey, Bothun, and Malin (1988, hereafter IBM). Surface photometry of Malin 1 reveals a very extended disk with a scale length of 55 kpc ($H_0 = 100 \text{ km s}^{-1} \text{ Mpc}^{-1}$) and a central surface brightness at V of 25.5 mag arcsec⁻². The luminosity of the disk is $M_V = -20.8$. The more prominent bulge component has an effective radius of 2.9 kpc and a total luminosity of $M_V = -19.5$. Spectroscopy of the nucleus shows strong [O II] $\lambda 3727$ emission and broad H α with a width of 5000 km s⁻¹. Other lines of high excitation are present such as [N II] $\lambda 6584$, and the spectrum is indicative of a high excitation Seyfert galaxy. Malin 1 has copious emission from the 21 cm line of neutral hydrogen, detected at the same velocity as the optical redshift. Including an uncertain correction for partial resolution, the H I mass is $\sim 10^{11} M_\odot$.

These are unprecedented properties for a spiral galaxy, but what makes Malin 1 particularly intriguing is that it was discovered by accident. The extremely low surface brightness disk is near the limit of the technique of photographic amplification

¹ Optical observations were obtained with the Multiple Mirror Telescope, a facility operated jointly by the Smithsonian Institution and the University of Arizona.

² Radio observations were obtained with the 43 m telescope at Green Bank, which is operated by Associated Universities, Inc., under contract with the National Science Foundation.

(Malin 1978), and only the unremarkable bulge is visible on UK Schmidt Sky Survey material. The nuclear emission lines proved that the galaxy was located far beyond the Virgo cluster and provided the crucial information needed to tune the 21 cm receiver to detect neutral hydrogen emission. The selection effects against discovering a galaxy such as Malin 1 are formidable. It is well known that existing galaxy catalogs are biased toward high surface brightness galaxies. In searches for the very faintest galaxies, the limitation imposed by sky brightness can be overwhelming (Disney 1976). IBM have quantified the effect of surface brightness on galaxy selection and on the shape of the Virgo galaxy luminosity function. Neutral hydrogen surveys in the 21 cm line do not compensate for the limitations of optical surveys. A large gas disk can evade detection at both high and low velocities when observed with the small beams and limited bandwidths of the most sensitive radio telescopes.

How unusual is Malin 1? The extremely low surface brightness disk has the largest scale length and the largest H I mass of any galaxy known. It is useful to identify galaxies that are similar to Malin 1 in that they share one or more of the following properties: low surface brightness disk, large mass, and large gas-to-star ratio. These "cousins" of Malin 1 are gathered together in Table 1. Columns (1), (2), and (3) list the object name, reference and description, and the heliocentric velocity is given in column (4). The physical parameters listed in columns (5)–(11) are the integrated H I mass, the width at 20% intensity of the 21 cm line, the total optical luminosity, the optical diameter from the UGC or ESO catalogs, the nuclear and extended $B-V$ colors, and the ratio of total H I mass to optical luminosity. All distance dependent quantities assume $H_0 = 100 \text{ km s}^{-1} \text{ Mpc}^{-1}$. Recently, Davies, Phillipps, and Disney (1988) have reported the discovery of a galaxy with an even lower surface brightness than Malin 1, but physical parameters cannot be derived for it without a redshift. None of the "cousins" in Table 1 approach Malin 1 in its striking combination of low surface brightness, large scale length and enor-

mous H I mass. Also, Malin 1 harbors the weakest active nucleus of the galaxies in Table 1, despite its abundant fuel supply.

In this paper, we present new observations of Malin 1, and a discussion of its relevance to galaxy formation and evolution and to the study of quasar absorption. Spectroscopic observations at radio and optical wavelengths are presented in § II, the H I properties are summarized in § III, and the nuclear spectrum is interpreted in § IV. The implications of Malin 1 for galaxy evolution and quasar absorption are discussed in §§ V and VI. Conclusions follow in § VII.

II. OBSERVATIONS

The unique feature of Malin 1 is the enormous H I disk, the spectrum of which was presented by BIMM. The Arecibo observations show a double-horned 21 cm profile at a systemic (heliocentric) velocity of $24,705 \text{ km s}^{-1}$, with a width at 20% intensity of 355 km s^{-1} . The asymmetry of both the H I profile and the optical nebulosity with respect to the nucleus indicate that some flux might have been missed by the Arecibo observation which was centered on the nucleus. Ideally, a 21 cm synthesis map of Malin 1 is required to map out the H I distribution. We are attempting to derive a rotation curve, using observations made recently at the VLA.

We have observed Malin 1 in the redshifted 21 cm line using the 140 foot (43 m) telescope at Green bank. The beam size of 22' is substantially larger than the Arecibo beam size of 3'. A total of 8 hr integration on the source was acquired using the L band receiver on the 140 foot telescope during the period 1987 November 27–30. The autocorrelator bandwidth was 10 MHz centered at $25,000 \text{ km s}^{-1}$. Total system temperature during the observations was $\sim 25 \text{ K}$. The off beam was located on a patch of sky which is sparsely populated down to the limit of a deep UK Schmidt plate. About 1 hr of data was omitted because of bad baselines due to interference from an elementary school thermostat, a worthy loss. A further hour of data

TABLE 1
COUSINS OF MALIN 1

Galaxy (1)	Reference (2)	Description (3)	v (km s^{-1}) (4)	M_{HI} (M_{\odot}) (5)	$\Delta v(20\%)$ (km s^{-1}) (6)	M_B (7)	Diameter (kpc) (8)	$B-V$ (nucleus) (9)	$B-V$ (total) (10)	M_{HI}/L_B (M_{\odot}/L_{\odot}) (11)
NGC 1512	1	Sb galaxy, interacting	714	2.8×10^9	250 ± 15	-17.7	33	...	0.87	1.4 ± 0.3
NGC 1079	2	S0 galaxy, faint disk	1460	1.1×10^9	380	-18.3	24	0.95	0.94	0.3
0016-579	3	S0 galaxy, faint disk	1629	2.2×10^9	265 ± 20	-16.8	17	0.58	0.88	2.7 ± 0.9
2010-373	3	S0 galaxy, faint disk	2538	5.3×10^9	465 ± 40	-19.2	32	1.00	0.96	0.7 ± 0.4
UGC 8253	4	LSB spiral	3264	1.0×10^9	145	-16.1	15	0.23	0.85	2.3
NGC 5291	5	S0 galaxy, interacting	4211	2.8×10^{10}	710 ± 10	-20.0	16	...	0.88	1.7 ± 0.3
NGC 5635	6	Sa galaxy, massive	4313	5.5×10^9	805	-19.8	21	0.44
UGC 542	7	LSB spiral	4510	8.6×10^9	350	-21.6	11	...	0.74	0.6
Mark 348	8	Seyfert 2, interacting	4757	1.0×10^{10}	930 ± 50	-19.1	28	0.95	0.86	0.82
UGC 6614	9	LSB spiral	6264	1.2×10^{10}	560	-20.0	55	0.98	0.75	0.85
NGC 3883	7	LSB spiral	7028	9.5×10^9	560	-21.3	67	...	0.89	0.4
UGC 12134	10	Sc galaxy	7389	3.0×10^{10}	507 ± 50	-20.0	35	0.78	0.64	1.8
0351+026	11	QSO, interacting	10357	1.3×10^{10}	1469 ± 100	-17.2	30	1.08	0.75	15
UGC 10	12	LSB spiral	11900	1.8×10^{10}	580	-20.2	62	1.05
UGC 9558	10	Sc I galaxy	13481	1.0×10^{10}	509	-20.7	32	...	0.72	0.38
UGC 9433	12	LSB spiral	13641	1.3×10^{10}	...	-20.8	59	0.43
I Zw 1	13	QSO, interacting	18285	1.3×10^{10}	360	-20.9	40	0.50	0.50	2.1
Malin 1	14	LSB spiral, active nucleus	24705	1.1×10^{11}	355 ± 10	-22.5	110	0.90	0.80	~ 3

REFERENCES.—(1) Harwarden *et al.* 1979; (2) Gallagher and Bushouse 1983; (3) Harwarden *et al.* 1981; (4) Romanishin *et al.* 1982; (5) Longmore *et al.* 1979; (6) Geller *et al.* 1989; (7) van der Hulst *et al.* 1987; (8) Heckman *et al.* 1982; (9) Bothun *et al.* 1985; (10) Bothun *et al.* 1984a; (11) Bothun *et al.* 1982; (12) Bothun, unpublished; (13) Bothun *et al.* 1984b; (14) BIMM and this paper.

was spoiled by local airborne radar. The remaining scans were baseline subtracted and co-added with weighting proportional to the inverse square of the noise on each scan. The resulting spectrum represents 6 hr of integration time, has an rms noise of ~ 2 mK, and is presented in Figure 1. A conversion of 3.4 mJy mK^{-1} was assumed, which is appropriate for a point source. Figure 1 shows the 21 cm spectrum from Green Bank as a solid line and the 21 cm spectrum from Arecibo as a dotted line. Both spectra are binned at 20 km s^{-1} resolution. The 140 foot data show residual interference due to airborne radar or oscillator harmonics at $25,220 \text{ km s}^{-1}$.

Only a short exposure optical spectrum was presented by BIMM. Therefore, we have reobserved the nucleus of Malin 1 using the Multiple Mirror Telescope (MMT) on Mount Hopkins. The MMT Spectrograph was used with a 3000 line grating blazed at $\sim 5000 \text{ \AA}$, giving a resolution of 5 \AA and a spectral coverage of 42000 \AA on the Reticon detector. The $1'' \times 3''$ slit was centered on the nucleus of the galaxy. Three separate observations were made with this setup: 160 minutes integration on 1987 February 19, 60 minutes integration on 1987 June 30, and 60 minutes integration on 1987 July 1. Sky conditions were photometric on these three nights, with average FWHM seeing profiles of $1''.5$, $1''.3$ and $1''.2$. The spectra were subjected to standard procedures of flat fielding, wavelength calibration and sky subtraction. The rms residual of the wavelength solution was 1.1 \AA . Individual 10 minute integrations were co-added weighted by their individual signal to noise ratio, in order to preserve the photon counting information from the Reticon detector. The spectra were corrected for extinction and for the heliocentric velocity correction. Calibration into absolute flux units was carried out with an observation of G-131 made on 1987 June 30. The spectrum of Malin 1 is shown in the upper panel of Figure 2, with the data rebinned in 4 \AA pixels, smoothed with a running 1-2-1 average,

and plotted in units of rest wavelength. For comparison of colors and line strengths, a 20 minute observation of the nucleus M87 was made with the same setup and at the same airmass. This is shown in the lower panel of Figure 2.

In collaboration with W. B. Latter and P. Maloney, a search for emission in the $J = 1 \rightarrow 0$ transition of CO from the nucleus of Malin 1 was made on 1988 May 18, using the NRAO 12 m telescope on Kitt Peak. At the redshift of Malin 1 the corresponding frequency is 105.730 GHz . The 12 m has a beam FWHM of $\approx 65''$ at this frequency. The observations were made using an SiS receiver and 1 MHz filter banks; the system temperature was 540 K during the observing period. No emission was detected: the 3σ upper limit for an rms of 5 mK and a 300 km s^{-1} FWHM is 0.44 K km s^{-1} .

Several additional observations were made in the vicinity of Malin 1. At the time of the MMT spectroscopy, it had been hoped to take spectra of the three blobs near the nucleus of Malin 1 which have the K-corrected colors of H II regions. The brightest of these is $V \sim 22$, and this proved an impossible task. However, with the aim of searching for off-nuclear H II regions or companion galaxies to Malin 1, we observed the three nearest condensations to the nucleus. These objects are visible on the finding chart in BIMM, they are labeled A, B, and C, and they have the following offsets from the nucleus: A, $7''$ W and $6''$ S; B, $25''$ W and $17''$ S; C, $32''$ W and $33''$ N. Spectra were obtained using the 300 line grating for A of 60 minutes exposure on 1987 June 28, for B of 90 minutes exposure on 1987 June 29, and for C of 60 minutes exposure on 1987 June 30. These spectra were rebinned in 8 \AA pixels, smoothed as described above, and are plotted in the three panels of Figure 3.

Finally, since the full extent of the gas and stars in Malin 1 is not known, we observed the nearest bright quasar to the galaxy at high spectral resolution. The quasar, H147 or

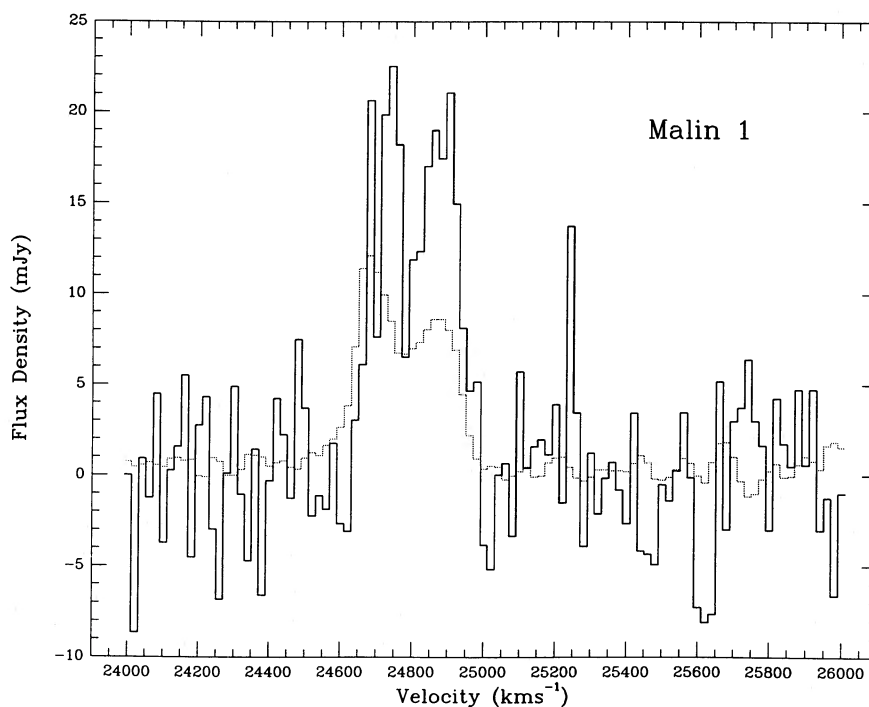


FIG. 1.—21 cm spectrum of Malin 1, with 43 cm Green Bank data plotted as a solid line, and 305 m Arecibo data plotted as a dotted line. Both spectra are binned at 20 km s^{-1} resolution.

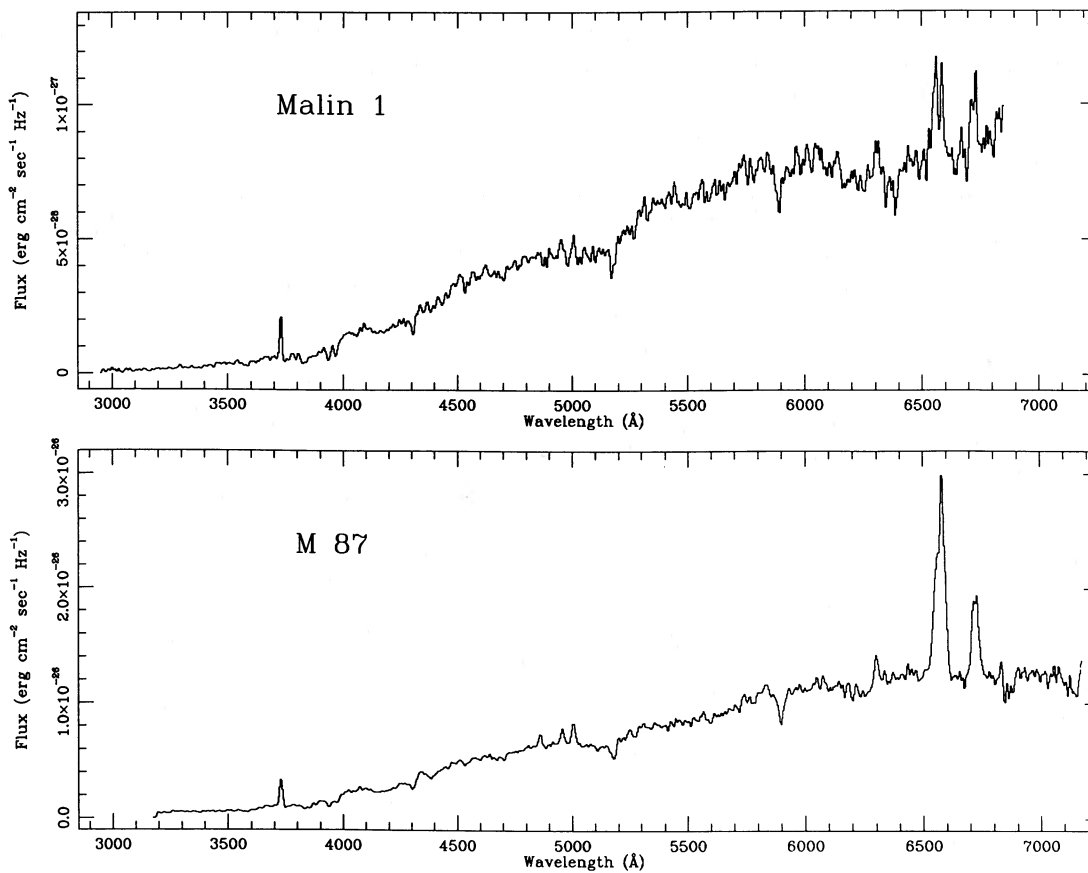


FIG. 2.—MMT spectra of (a) Malin 1 and (b) M87, plotted in flux units. Both spectra have 5 Å resolution, taken with a 300 line grating.

1234 + 145, was discovered in an automated machine survey of objective prism plates of the Virgo region using the APM at Cambridge, England (P. Hewett, private communication). It is located at $12^{\text{h}}34^{\text{m}}0^{\text{s}}.16$, $+14^{\circ}29'45''.6$ (1950), with $z = 1.601$ and $V = 18.5$. An integration of 160 minutes with the 800 line grating at 2 Å resolution on 1988 January 14 was followed by an integration of 120 minutes with the 832 line grating (used in second order) at 1 Å resolution on 1988 February 21. These spectra were binned in 1.5 and 0.75 Å pixels, smoothed and are plotted in Figure 4. The spectra are centered on the wavelengths of Ca II H and K at the redshift of Malin 1. An associated C IV $\lambda 1548, 1550$ doublet was found at a recession velocity of ~ 2000 km s $^{-1}$ from the quasar emission redshift; the absorption system is marked in Figure 4. While the search for absorption at a projected distance of ~ 600 kpc from a spiral galaxy is clearly optimistic, the large inferred sizes of quasar heavy element absorbers and the extraordinary nature of Malin 1 makes the observation worthwhile. A journal of observations is presented in Table 2, with object name, telescope, U.T. date of observation, wavelength and resolution of the data, and integration time in columns (1)–(6).

III. H I PROPERTIES OF THE DISK

a) Characteristics of Malin 1

Malin 1 is remarkable for the mass of its neutral material. The H I profile is characteristic of a rotating disk of gas. Figure 1 shows that the H I diameter is significantly larger

than 240 kpc, because the flux integrals from the NRAO 140 foot and the Arecibo dish differ. The flux integral under the line is $\int S_{\nu}(v)dv = 4.6$ Jy km s $^{-1}$ for the NRAO data and 2.7 Jy km s $^{-1}$ for the Arecibo data. The Arecibo flux integral is different from that quoted by BIMM because a different baseline was fitted when the spectrum was rebinned. However, these numbers are equal within the errors, given the uncertain flux calibration at this frequency and the unknown mass distribution of the disk. The two peaks in the Green Bank data are more symmetric than the peaks in the Arecibo data, another indication that little flux is being missed by the larger beam. A follow-up observation in 1987 June with the Arecibo dish pointed 1' south of the nucleus of Malin 1 gave a flux integral of 2.5 Jy km s $^{-1}$, and velocity widths of $\Delta V_{20} = 357$ km s $^{-1}$ and $\Delta V_{50} = 300$ km s $^{-1}$. Therefore the H I emission is predominantly centered on the optical nucleus. The observed H I mass is $M_{\text{H I}} = 2.36 \times 10^5 \int S_{\nu}(v)dv D(\text{Mpc})^2 = 6.7 \times 10^{10} M_{\odot}$. All other derived H I parameters are uncertain because of the unknown disk inclination and the limitations of a single beam measurement, but even rough estimates are informative. Neutral hydrogen properties are summarized in Table 3, where the good agreement between the Arecibo (col. [2]) and Green Bank (col. [3]) measurements can be seen. In Table 3, v_{sys} is the mean velocity between the 20% power points of $S_{\nu}(v)$, v_{min} is the position of the dip in the two-horned profile, and the lower three parameters in the table assume a correction for partial resolution.

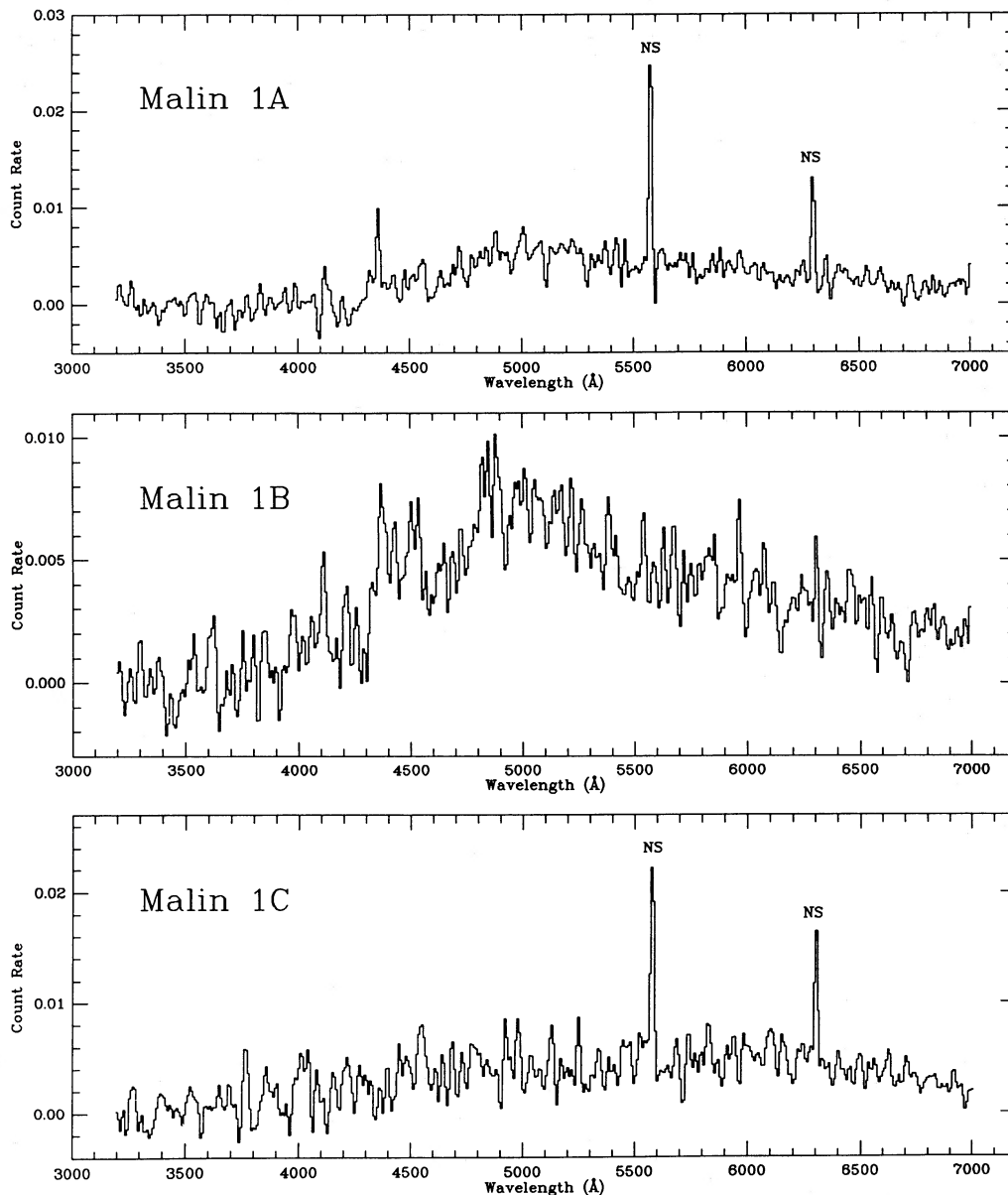


FIG. 3.—MMT spectra of (a) Malin 1A, (b) Malin 1B, and (c) Malin 1C, three condensations near Malin 1. The spectra are binned at 8 Å resolution and are not flux calibrated. Residual night sky lines are marked NS.

The broad two-horned H I profile is atypical for a face-on system. Lewis (1987) has studied the H I profiles of face-on spiral galaxies, and only 1% with $i < 30^\circ$ have $\Delta V_{20} > 350 \text{ km s}^{-1}$. A weaker constraint on the inclination comes from the CCD image in BIMM. The distribution of nebosity in the low surface brightness disk makes it unlikely that $i > 60^\circ$. Taking $i \sim 45^\circ$ as an estimate, we derive a corrected 21 cm line width of $W_0 = (\Delta V_{20} + \Delta V_{50})/2 \sin i(1+z) = 420 \text{ km s}^{-1}$, following the definition of Haynes and Giovanelli (1984). The total H I mass corrected by a factor of 1.6 for the partial resolution of the Green Bank measurement is $1.1 \times 10^{11} M_\odot$. The mean column density of H I is $\sim 2 M_\odot \text{ pc}^{-2}$ or $\sim 2 \times 10^{20} \text{ H atoms cm}^{-2}$, which is a lower limit if the H I extent is significantly smaller than the Arecibo beam. However, the excess flux observed in the 140 foot beam indicates that H I disk is larger than 3.3.

The H I properties of Malin 1 can be compared with the sample of isolated galaxies studied by Haynes and Giovanelli (1984). The total mass is derived from an assumed rotation law (usually a flat Brandt law), and 80% of the isolated galaxies have ratios of H I to total mass in the range $1.2 < \log (M_T/M_{\text{HI}}) < 2.2$. If Malin 1 follows such a curve, then the peak of the rotation curve will lie between 0.5 and 5 kpc (or less than 4") from the nucleus, giving a value of $M_T/L_B \sim 80$. A comparison between the H I/optical properties of Malin 1 and other galaxies is complicated by the extreme low surface brightness of the disk. If $(B-V) \sim 0.5$, the Holmberg diameter of the disk is vanishing. Haynes and Giovanelli (1984) found that the diameter of a spiral disk is a good indicator of the H I mass. Clearly, this is *only* true if the dependence on optical surface brightness is also considered. If the optical luminosity is a good indicator of the H I velocity width (Tully and Fisher

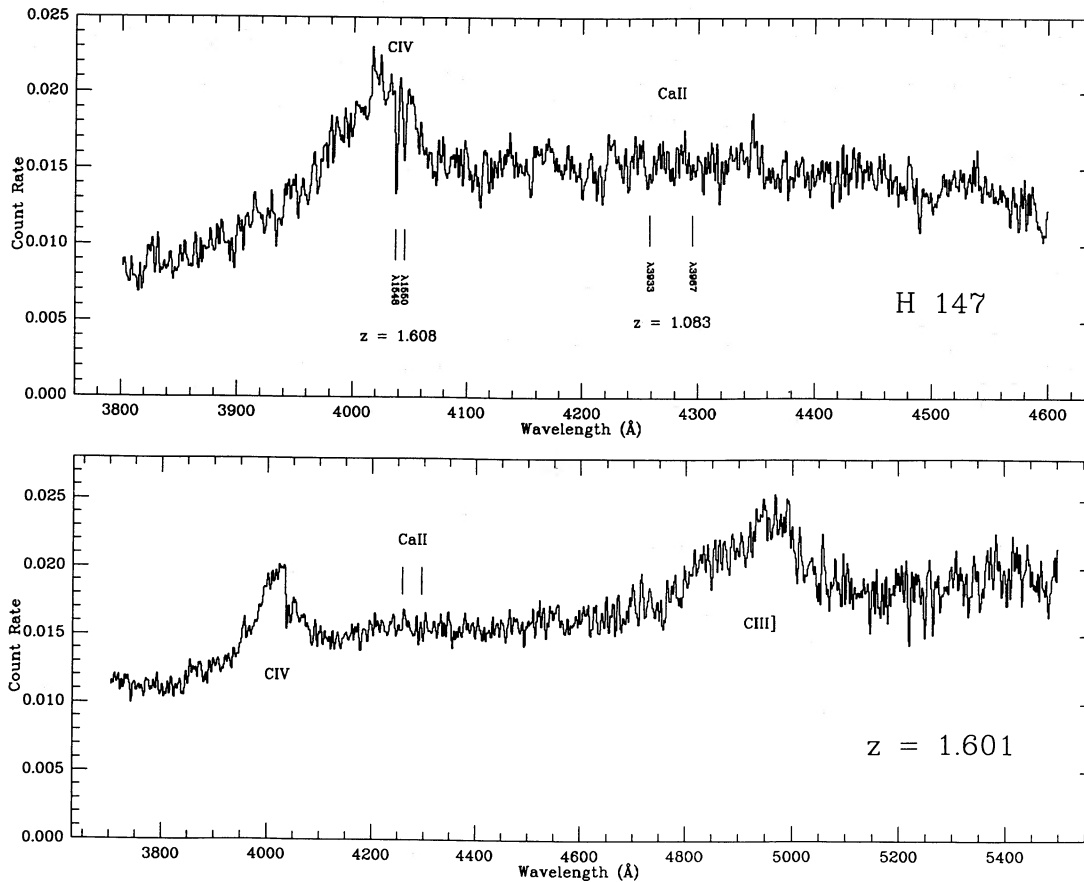


FIG. 4.—MMT spectra of the quasar H147 near Malin 1. The upper panel has 2 Å resolution (800 line grating), the lower panel has 1 Å resolution (832 line grating, second order).

1977), then the inclination of the Malin 1 disk should be $\sim 25^\circ$. The integrated light in the exponential disk gives $M_o = -20.8$ or $L_B = 2.6 \times 10^{10} L_\odot$. The bulge contributes an additional $L_B = 1 \times 10^{10} L_\odot$, giving an integrated gas-to-stars ratio of $M_{HI}/L_B \sim 3$.

We can also interpret the limit on CO emission, obtained in collaboration with W. B. Latter and P. Maloney on the NRAO 12 m telescope. At the assumed distance of Malin 1, the 12 m beam covers an area of 4100 kpc². The upper limit on the intensity of the CO $J = 1 \rightarrow 0$ line thus corresponds to an upper limit on the CO luminosity of $L_{CO} \leq 2100 \text{ K km s}^{-1}$

kpc². If we assume that the conversion between CO luminosity and mass of molecular hydrogen is the same as derived for the Galaxy from comparison of the COS B gamma-ray data with the GISS CO survey (Bloemen *et al.* 1986), we derive an upper limit to the mass of H₂ in the 12 m beam of $8.4 \times 10^9 M_\odot$. This is 12 times smaller than the mass of atomic hydrogen. However, since the distributions of molecular and atomic hydrogen are ordinarily very different in spiral galaxies, with the H₂ concentrated in the inner regions of the galaxy and the atomic hydrogen in a flat extended disk, this upper limit does not place a strong constraint on the relative masses of molecu-

TABLE 2
JOURNAL OF OBSERVATIONS

Object (1)	Telescope (2)	Date (U.T.) (3)	Wavelength Range (4)	Resolution (5)	Internal Time (s) (6)
Malin 1	NRAO 43 m	1987 Nov 27–30	19.44–19.57 cm	4 km s ⁻¹	21600
Malin 1	MMT	1987 Feb 19	3200–7400 Å	5 Å	9600
Malin 1	MMT	1987 Jun 30	3200–7400 Å	5 Å	3600
Malin 1	MMT	1987 Jul 1	3200–7400 Å	5 Å	3600
M87	MMT	1988 Feb 21	3200–7200 Å	5 Å	600
Malin 1A	MMT	1987 Jun 28	3200–7000 Å	5 Å	3600
Malin 1B	MMT	1987 Jun 29	3200–7000 Å	5 Å	5400
Malin 1C	MMT	1987 Jun 30	3200–7000 Å	5 Å	3600
H147	MMT	1988 Jan 14	3600–5600 Å	2 Å	9600
H147	MMT	1988 Feb 21	3800–4600 Å	1 Å	7200

TABLE 3
H I PROPERTIES

Property (1)	NRAO 43 m (2)	Arecibo 305 m (3)
v_{sys} (km s $^{-1}$)	24745	24705
v_{min} (km s $^{-1}$)	24715	24710
ΔV_{20} (km s $^{-1}$)	340	355
ΔV_{50} (km s $^{-1}$)	315	295
$\int S_{\nu}(v)dv$ (Jy km s $^{-1}$)	4.6	2.7
$M_{\text{H I}}$ (M_{\odot})	1.1×10^{11}	
$\langle \sigma_{\text{H I}} \rangle$ (cm $^{-2}$)	$\sim 2 \times 10^{20}$	
$M_{\text{H I}}/L_B$	~ 3	

lar and atomic hydrogen within the NRAO beam. Furthermore, it is not clear that molecular clouds in Malin 1, if they are present, will have properties similar to Galactic molecular clouds that use of the Galactic conversion factor is justified. Because the rate of star formation in Malin 1 is so low, both the intensity of the average interstellar radiation field and the cosmic-ray flux will be considerably reduced from the Galactic values. Thus the average temperature of molecular gas may be considerably lower than is typical for Galactic clouds, so that the amount of molecular hydrogen present in Malin 1 could be underestimated by the use of a Galactic conversion factor, which implicitly assumes that the molecular clouds have gas kinetic temperatures of ~ 10 K. If Malin 1 has been forming stars at a very low rate in its disk throughout its lifetime, the metallicity of the gas may be very low, which would also lead to an underestimate of the molecular gas from the CO emission alone. Although the paucity of current star formation in Malin 1 suggests that molecular gas is not present in abundance, it is very difficult to quantify this with presently available CO observations.

b) Comparison with Normal Disk Galaxies

Malin 1 is exceptional in terms of total H I mass, optical luminosity, optical size, and ratio of gas to stars. It is modest only in its *surface mass density* of gas and stars. This is the important clue to the nature of Malin 1. Our reference for the detailed H I properties of spiral galaxies is the study of Virgo cluster spirals by Warmels (1988*a, b, c*). Warmels used aperture synthesis measurements with the Westerbork telescope to map out the radial gradients in H I surface density. To the 18 galaxies with the best-quality data in his sample we add Malin 1 and four of its "cousins" with H I data, NGC 3883 and UGC 542 from van der Hulst *et al.* (1987), and 0016–579 and 2010–373 from Hawarden *et al.* (1981). The four cousins share with Malin 1 the properties of very low surface brightness disks and high values of $M_{\text{H I}}/L_B$. All of these galaxies except Malin 1, 0016–579, and 2010–373 have neutral hydrogen synthesis maps. It is likely that a clear understanding of star formation in disk galaxies will require two-dimensional data, since the global parameters of $M_{\text{H I}}$, L_B , and $M_{\text{H I}}/L_B$ often mask large and important variations in the surface mass densities of gas and stars.

The values of $M_{\text{H I}}/L_B$ and mean H I column density $\langle \sigma_{\text{H I}} \rangle$ are plotted in Figure 5. The mean H I column density for the galaxies with synthesis maps is calculated over the area above the detection threshold ($2\text{--}4 \times 10^{19}$ cm $^{-2}$). For the two galaxies from Hawarden *et al.* (1981), the mean surface density is defined over the Holmberg diameter, and for Malin 1 it is defined over the area of the Arecibo beam. Malin 1 and its four cousins have unusually high H I mass-to-light ratios and unusually low mean H I surface densities. This is expected in the case of very slowly evolving disk galaxies, if $\sigma_{\text{H I}}$ controls the time scale between episodes of star formation. During the lulls between episodes of star formation, the disks of these galaxies may fade (and redden), thus increasing the apparent gas-to-star ratio (Schommer and Bothun 1983). All of the low surface brightness galaxies have $M_{\text{H I}}/L_B > 0.33$, compared

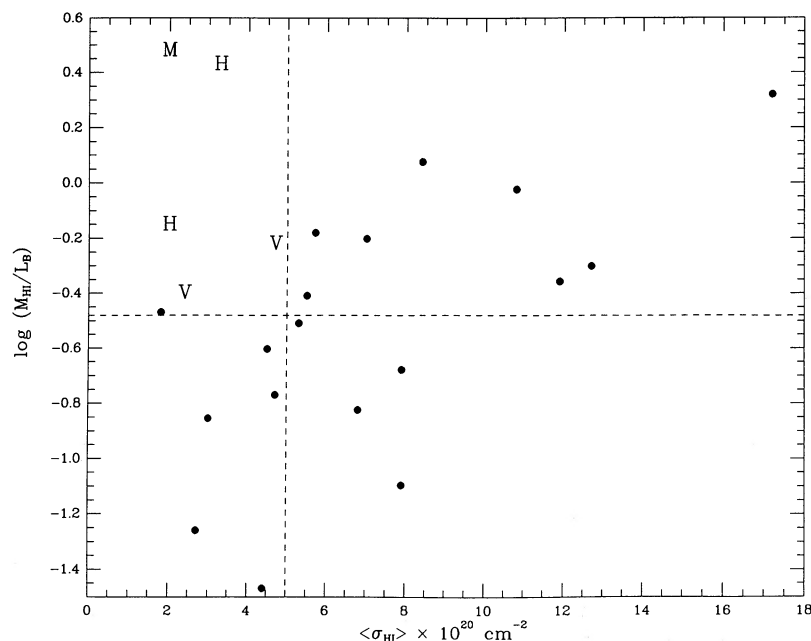


FIG. 5.—The ratio of H I mass to blue luminosity plotted against mean H I surface density for 23 spiral galaxies. Shown are 18 Virgo spirals from Warmels (1988; filled circles), two galaxies from van der Hulst *et al.* (1987; V symbols), 2 galaxies from Hawarden *et al.* (1981; H symbols), and Malin 1 from this paper (M symbol).

with only 40% of the normal Virgo spirals. The low surface brightness galaxies are also extreme in total mass to light. The Virgo spirals have a range of $M_T/L_B = 4.6 \pm 2.1$, compared to values of 12 and 19 for the two low surface brightness galaxies with rotation curves. The other three low surface brightness galaxies have more uncertain values in the range $20 < M_T/L_B < 80$. Virgo spirals with $M_{HI}/L_B > 0.33$ have a mean column density $\langle \sigma_{HI} \rangle = 9.9 \pm 4.1 M_\odot \text{pc}^{-2}$, while Malin 1 plus cousins have $\langle \sigma_{HI} \rangle = 2.9 \pm 1.1 M_\odot \text{pc}^{-2}$. As pointed out by van der Hulst *et al.* (1987), the low surface mass density of H I is probably crucial in understanding galaxies like Malin 1 and its relatives. Integrated quantities such as M_{HI} and L_B are less informative, for while Malin 1 has an enormous total mass of gas and stars, the masses of the two low surface brightness disk galaxies of Hawarden *et al.* (1981) are unexceptional.

c) A Threshold for Star Formation

Most work on the global star forming properties of galaxies has assumed a monotonic dependence of star formation rate on gas density (Schmidt 1959). However, the details and physical basis of such a smooth relationship have been hotly debated (Freedman 1984; Kennicutt *et al.* 1987; Young and Scoville 1982). At low gas densities, it is reasonable to expect a *threshold* in the star formation process, based on the density at which the gas in a rotating disk becomes unstable to shear forces (Goldreich and Lynden-Bell 1965; Quirk 1972). Quirk derived a critical density for the onset of star formation as a function of κ , the epicyclic frequency in $\text{km s}^{-1} \text{kpc}^{-1}$. Using the solar neighborhood for the calibration from volume to surface mass density, and assuming an arm/interarm density contrast of a factor of 2, he deduced that $\sigma_{crit} \sim 0.3 \times 10^{20} \kappa \text{ H atoms cm}^{-2}$. Comparison with the few existing rotation curves showed that the observed surface densities in the outer parts of four galaxies followed the predicted threshold well. The inner

parts were observed to be well below the predicted threshold, although if the molecular gas is included, surface densities are close to the critical value over a large range of radius (R. C. Kennicutt, private communication).

We repeat the Quirk analysis for the spirals with good rotation curves published by Warmels (1988c) and van der Hulst *et al.* (1987), taking $\kappa = [2v_r/r(v_r/r + \delta v_r/\delta r)]^{1/2} \text{ km s}^{-1} \text{ kpc}^{-1}$, and calculating $\sigma_{HI}/\sigma_{crit}$ as a function of radius. As found by Quirk, the values of $\sigma_{HI}/\sigma_{crit}$ decrease at small radii. The galaxies define parallel tracks in σ_{HI} versus σ_{crit} (as a function of radius), with values covering the large range of $0.06 < \sigma_{HI}/\sigma_{crit} < 2.5$. However, the data plotted in Figure 6 shows that the values of $\sigma_{HI}/\sigma_{crit}$ defined at the Holmberg radius increase with increasing M_{HI}/L_B . The same result is found if metric diameters defined at 10 kpc are used instead of isophotal diameters. Figure 6 demonstrates a significant connection between a global property of the galaxy, M_{HI}/L_B , and the proximity of the galaxy to the calculated threshold for star formation, $\sigma_{HI}/\sigma_{crit}$. Note that all of the galaxies with $M_{HI}/L_B > 0.4$ (i.e., the galaxies with the lowest mean surface densities in Fig. 5), are also those within a factor of 2 of the threshold surface density in their outer regions. From the low mean surface densities of Malin 1 and the two Hawarden *et al.* galaxies, we would expect them also to lie at or below the star formation threshold. Bothun (1982) has shown that M_{HI}/L_B is a rapidly evolving quantity in the case of continued star formation. Therefore, we expect this parameter to exhibit a static behavior when the surface density nears the critical value.

The concept of a threshold for star formation appears to be relevant to spiral galaxies over a wide range of sizes and luminosities (Gallagher and Hunter 1984). Malin 1 and its cousins represent an important extension of known galaxy properties in the direction of low optical surface brightness, low H I surface density, and high M_{HI}/L_B . These properties appear to be related. Galaxies with high M_{HI}/L_B have outer parts that

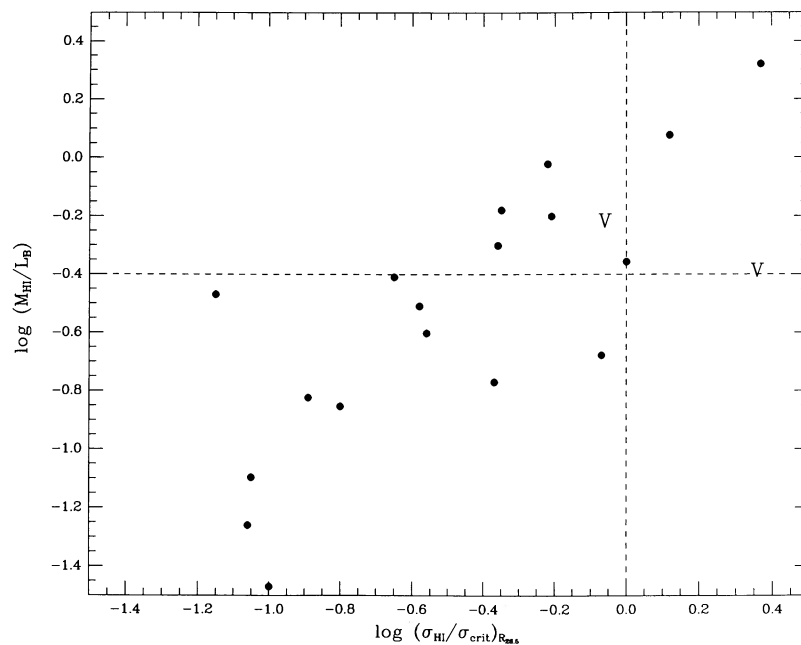


FIG. 6.—The ratio of H I mass to blue luminosity plotted against the ratio of H I surface density to critical surface density (defined at the Holmberg radius). Critical surface density is calculated from the rotation curve, using the prescription of Quirk (1972). Symbols as in Fig. 5.

are close to the critical surface density for stability to gravitational contractions in a rotating H I disk. The evidence indicates the existence of massive galactic systems whose importance and prevalence have been underestimated because they lie below the threshold for active star formation.

IV. STELLAR POPULATION OF THE BULGE

a) Energy Distribution

The disk of Malin 1 is extremely faint, so it is difficult to derive optical constraints on the stellar population. The bulge is bright enough for a discussion of stellar populations, based on the spectrum in Figure 2. In particular, we are interested in how the bulge of Malin 1 relates to the bulges of other spirals, and to the old stellar populations in E and S0 galaxies. Although the bulge-to-disk luminosity ratio of Malin 1 is not very large, the disk has such low surface brightness that our nuclear spectrum measures primarily the bulge component. Using the decomposition into bulge and disk from BIMM, the disk contributes only $\sim 2\%$ to the spectrum of Malin 1 in Figure 2.

The only information on the energy distribution of Malin 1 is at optical and near infrared wavelengths. There is an upper limit of 60 mJy to the radio flux at 5 GHz from the MIT-Green Bank (MG) survey (Bennett *et al.* 1986). As reported by BIMM, Malin 1 is not detected in a co-add of the IRAS survey data base; the 3σ upper limits are 112 mJy ($12\ \mu\text{m}$), 146 mJy

($25\ \mu\text{m}$), 140 mJy ($60\ \mu\text{m}$), and 380 mJy ($100\ \mu\text{m}$). The lack of a far infrared detection is not surprising due to the modest luminosity of the nuclear source.

In collaboration with G. Neugebauer, C. D. I. has measured the near-infrared colors of the nucleus of Malin 1 using an InSb photometer on the Palomar 200 inch telescope. The following flux densities were obtained through a $4''$ aperture: 2.0 ± 0.2 mJy ($1.25\ \mu\text{m}$), 2.5 ± 0.2 mJy ($1.65\ \mu\text{m}$), 2.3 ± 0.2 mJy ($2.2\ \mu\text{m}$), < 1.9 mJy ($3.7\ \mu\text{m}$). The corresponding colors reduced on the system of Elias *et al.* (1982) are $(J-H) = 0.72 \pm 0.10$, $(H-K) = 0.40 \pm 0.10$, $(K-L) < 0.88$. These results can be compared with the mean colors of elliptical galaxy nuclei from Impey, Wynn-Williams, and Becklin (1986): $(J-H) = 0.75$, $(H-K) = 0.20$, $(K-L) = 0.32$. While the $(J-H)$ color of Malin 1 is typical of early-type galaxies, the $(H-K)$ color is 0.25 mag redder than the colors of late-type giants. Unfortunately, we cannot use the infrared colors to draw conclusions about stellar populations, since we do not know the contribution of the AGN component at long wavelengths.

BIMM derive $(B-V)$ colors of 0.90 ± 0.02 in a $20''$ aperture and 0.95 ± 0.02 in a $4''$ aperture, the numbers derived from CCD surface photometry. Colors can be derived from the flux calibrated spectrum in Figure 2, by convolving the energy distribution with the appropriate filter response. For Malin 1 in an effective $2''$ aperture, the color is $(B-V) = 1.20 \pm 0.02$, where the color has been corrected for redshift and the error is derived from counting statistics. The color for M87 derived

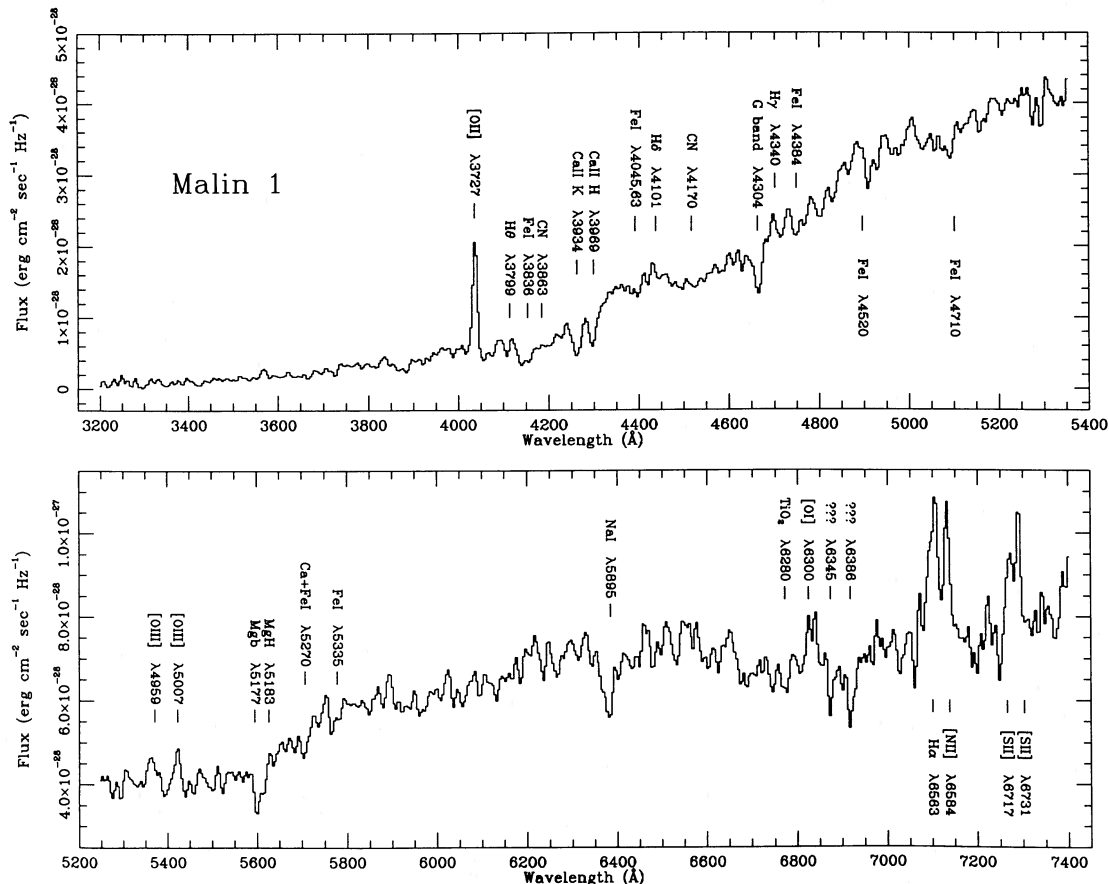


FIG. 7.—MMT spectrum of Malin 1, plotted in flux units with principal absorption and emission features marked

TABLE 4
 EMISSION AND ABSORPTION LINES

Line (1)	Wavelength (Å) (2)	Line Flux (ergs s ⁻¹ cm ⁻²) (3)	Equivalent Width (Å) (4)	FWZI (km s ⁻¹) (5)
[O II]	λ3727	2.5 × 10 ⁻¹⁶	21.9 e	1600
Ca II K	λ3933	...	9.7 a	...
Ca II H	λ3967	...	6.5 a	...
G band	λ3404	...	8.0 a	...
[O III]	λ4959	9.5 × 10 ⁻¹⁷	2.2 e	...
[O III]	λ5007	7.0 × 10 ⁻¹⁷	1.7 e	...
Mg I	λ5180	...	5.0 a	...
Na I	λ5895	...	5.8 a	...
[O I]	λ6300	2.1 × 10 ⁻¹⁶	4.8 e	...
Hα + [N II]	λ6563, 6584	6.9 × 10 ⁻¹⁶	15.4 e	5800
[S II]	λ6717, 6731	3.2 × 10 ⁻¹⁶	7.1 e	...

from spectroscopy is $(B-V) = 1.06$, in agreement with the value of 1.01 measured through a similar effective aperture from the surface photometry of Young *et al.* (1987). Since the method of deriving colors from spectra reproduces standard star colors and the nuclear color of M87, we believe that the extreme redness of the Malin 1 nucleus is real.

b) Line Indices

The main features of the optical spectrum are labeled in Figure 7. Apart from the unusually red continuum, all the normal absorption features typical of an old stellar population are seen. In particular, strong CN bands and Fe I features occur in the blue; while MgH, Na I and at least one TiO band are prominent in the red part of the spectrum. Very weak Balmer lines Hδ λ4101 and Hγ λ4340 are seen in emission. The emission is dominated by strong and broad Hα, strong lines of [O II], [N II], and [S II], and relatively weak [O III]. A list of the prominent emission and absorption lines is given in Table 4, with line fluxes, equivalent widths, and velocity widths in columns (3), (4), and (5). Absorption line indices are listed in Table 5, with the line-to-continuum (L/C) ratio plus error for Malin 1 in columns (3) and (4), and L/C for M87 in column (5). References for the definition of the indices are in column (6). The errors in the Malin 1 indices are calculated from the rms repeatability of the three separate observations.

Our aim is to define the stellar population in the bulge of Malin 1 and compare it with the population in less exotic galaxies. Boroson (1980) has studied the abundances of spiral bulges and ellipticals using two narrow line indices. His Mgb index measures the atomic Mg triplet and the MgH bandhead and is similar to the Mg_2 index defined by Faber (1977). His CN 39 index measures the strength of the broad trough due to CN around 3860 Å. Figure 8 shows data for spiral bulges and ellipticals taken from Boroson (1980), with Malin 1 added. Like many of the spiral nuclei, Malin 1 has too weak a CN 39 index for its metallicity (presumed to be indicated by Mg b). Boroson accounted for this effect with the addition of a bulge continuum due to hot O to F main-sequence stars. Using his prescription, we calculate that the fraction of light 4500 Å coming from young stars earlier than G0 is ~30%, and that the value of Mgb corrected back to the mean metallicity relation for ellipticals is $(Mgb)_c = 0.34$. This hot star fraction is similar to that derived for M32 using his method. Boroson has presented reasons why this hot component must be due to recent star formation rather than metal-poor horizontal

branch stars. In the next section, we argue that the weakness of CN 39 is *not* due to dilution by a power-law component responsible for photoionizing the emission line region.

Figure 9 shows the location of Malin 1 on a metallicity (Mgb) versus luminosity (M_B) diagram, with data on spiral bulges and ellipticals from Boroson (1980). Malin 1 lies close to the mean metallicity-luminosity relation for ellipticals and at the upper end of the metallicity and luminosity range (no correlation is evident) for spiral bulges. It is pointed out that S0 nuclei are not distinguishable from ellipticals in terms of their line strengths or colors (Gregg 1985). The evidence for young stars Malin 1 indicates that its nucleus is more closely allied to spiral bulges than S0 nuclei. Such a conclusion is important, because Boroson (1980) has argued that the disk material in spirals has little influence on the processes which affect star formation in the bulge.

The bulge stars in Malin 1 can be compared with old stellar populations. We have measured the 10 absorption line indices defined by Burstein *et al.* (1984) and find that Malin 1 lies at the high metallicity end of the mean relationships defined by 170 elliptical galaxies and has substantially higher metallicity than the sequences defined by galactic and M31 globular clusters. Malin 1 is within 2 σ of the mean elliptical galaxy relation for all 10 indices; however, the displacement is always in the sense of having too weak absorption for the metallicity (value of

 TABLE 5
 ABSORPTION LINE INDICES

LINE (1)	CENTRAL WAVELENGTH (2)	MALIN 1		M87 L/C (5)	REFERENCE (6)
		L/C (3)	$\sigma(L/C)$ (4)		
Ca II K	λ3933	0.711	0.152	0.753	1
Hδ	λ4101	1.000	0.038	1.045	1
Ca I	λ4226	0.969	0.060	0.964	1
G band	λ4304	0.779	0.046	0.888	1
Fe I	λ4383	0.970	0.018	0.986	1
He I	λ4471	1.075	0.021	1.060	1
TiO	λ4960	0.935	0.020	...	1
Mg I	λ5183	0.935	0.039	0.895	1
Mg H	λ5208	0.958	0.052	0.963	1
Na I	λ5892	0.910	0.089	0.865	1
Mg b	λ5177	0.761	0.050	0.766	2
CN 39	λ3860	0.609	0.059	0.624	2

REFERENCES.—(1) Williams 1976; (2) Boroson 1981.

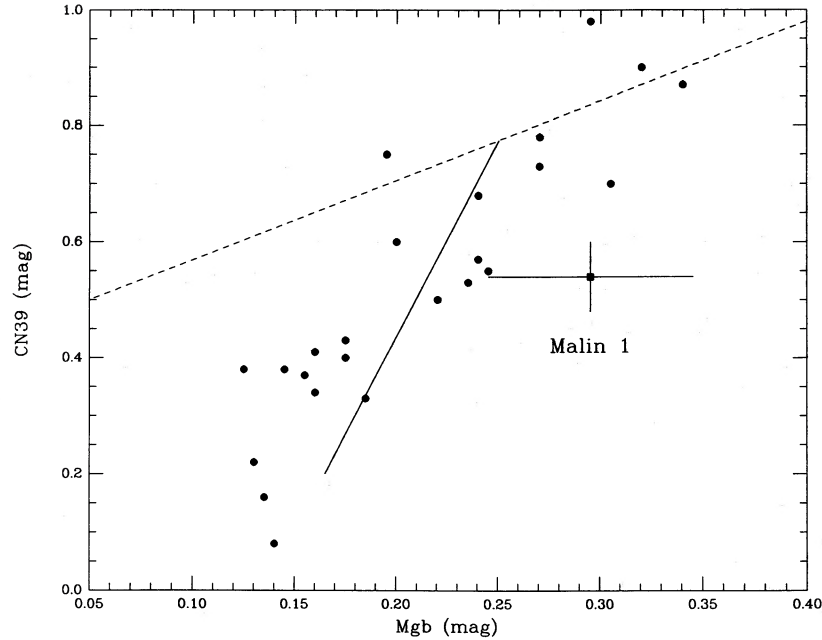


FIG. 8.—CN 39 and Mgb indices plotted for 24 spiral bulges from Boroson (1980), along with the mean relationship for elliptical galaxies (*dashed line*). Malin 1 is shown as a square, with error bars derived from the repeatability of three separate observations. The solid line is the vector for the addition of a hot star component, from Boroson (1980).

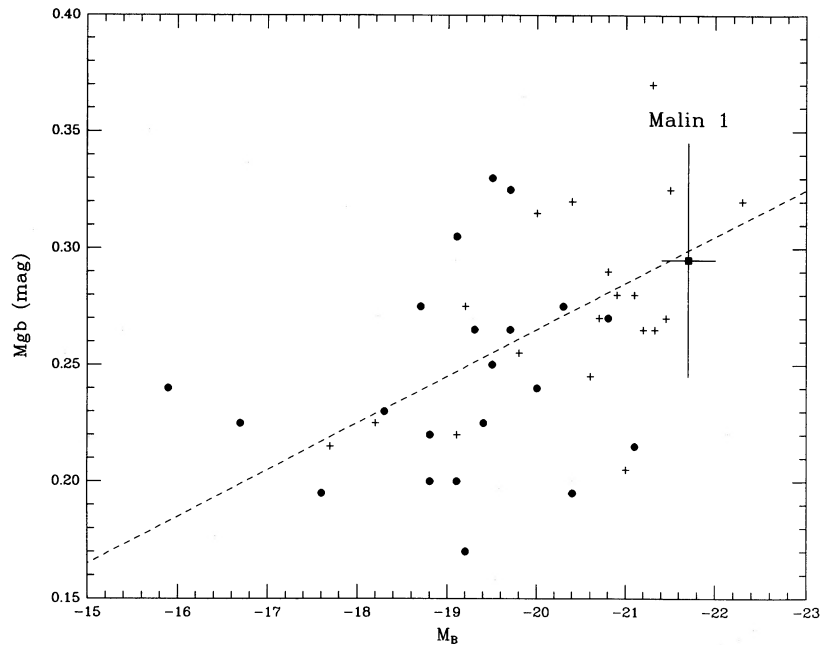


FIG. 9.—The Mgb index plotted against blue luminosity for spiral bulges (*filled circles*) and ellipticals (*crosses*) from Boroson (1980). The mean relationship for ellipticals is shown as a dashed line, and Malin 1 is included as a square.

(M_2). As Burstein and his collaborators have made painfully clear, it is exceedingly difficult to use spectral features to tie down the age and metallicity of an old stellar population. Malin 1 therefore becomes a microcosm of the complex problems in stellar synthesis. To summarize, we see a predominantly old stellar population, with some evidence for young stars from the weak Balmer lines in emission and weak CN 39.

c) The Active Nucleus

For a galaxy with such an abundant supply of gas, Malin 1 has produced a particularly modest active nucleus. The emission lines in Figure 2 are typical of a Seyfert 1 galaxy. The diagnostic line ratios of $[N II] \lambda 6584/H\alpha = 1.0$ and $[O III] \lambda 5007/H\beta = 4.8$ place the nucleus of Malin 1 firmly in the

region of photoionization by a power-law continuum (Baldwin, Phillips, and Terlevitch 1981). Due to the unknown age, metallicity, and reddening, the continuum cannot be uniquely decomposed into a stellar continuum and a power law. This raises the question of whether the evidence for young stars from Figure 8 is secure, or if the weakness of CN 39 could be explained by a power law contributing in the blue. A power law that contributes 30% of the flux at 4000 Å contributes only 4% ($\alpha = 1$) or at most 6% ($\alpha = 2$) of the flux at 5600 Å. Therefore, a single power-law component cannot simultaneously account for the weakness of CN 39 and the absorptions at Mg H and Na I. The broad H α line has a FWZI of 5800 km s⁻¹, roughly at the boundary of the range of line widths for Seyfert 1 and 2 galaxies (Osterbrock 1977). The steep Balmer gradient and large H α /H β ratio is more typical of a BLRG than a Seyfert 1. Fe II emission around 4500 Å and 5300 Å is unusually weak.

Malin 1 has the fuel supply, gas motions, and excitation of a powerful active nucleus, yet the broad-line luminosity is very modest. The H α + [N II] equivalent width is only 15 Å, which is the media nuclear equivalent widths of a field sample of S0/Sa galaxies (Kennicutt *et al.* 1987). Only 5% of such a sample of field galaxies have Seyfert ionizations, and none of them have the broad lines typical of a Seyfert 1. From the luminosity function of Meurs and Wilson (1984), only 2% of galaxies with the blue luminosity of Malin 1 harbor Seyfert nuclei, and less than half of those have the broad lines and high excitation of a Seyfert 1 galaxy. The nucleus of Malin 1 is at only the fifth percentile of the Seyfert 1 luminosity function. The velocity width of H α in Malin 1 is larger than the widths of H α in all the spirals studied by Keel (1983). However, the H α + [N II] luminosity is at a level where nuclear activity becomes ubiquitous in spirals. Presumably the puniness of the active nucleus in Malin 1 is due to a low feeding rate.

V. IMPLICATIONS FOR GALAXY EVOLUTION

a) Environment of Malin 1

An enormous gas disk as expected will be fragile with respect to encounters with other galaxies, so we have studied the neighborhood of Malin 1. One of the three condensations close to the nucleus shows weak evidence for being an early-type galaxy at $\sim 22,500$ km s⁻¹ (Fig. 2b). The velocity derived from the cross-correlation technique of Tonry and Davis (1979) has a third of the correlation peak of the cross-correlation velocity derived for Malin 1. The only convincing feature is the redshifted 4000 Å break; another spectrum is needed to confirm this result. In two dimensions, the area of sky around Malin 1 has very few faint ($V > 19$) galaxies that might be companions. In three dimensions, John Huchra (CfA) has been carrying out a galaxy redshift survey that probes the volume around Malin 1. For example, Huchra and Brodie (1984) have discovered a poor cluster of galaxies behind M87 at a velocity of $\sim 25,800$ km s⁻¹. Malin 1 is ~ 17 Mpc for this grouping. Although the volume at high velocities is only sampled for luminous galaxies, we note that behind the Virgo cluster in the velocity range $25,000 \pm 4000$ km s⁻¹ there is about one galaxy 2500 Mpc⁻³. The empty volume around Malin 1 before a nearest neighbor is reached is 9200 Mpc³; therefore it is likely that Malin 1 is in a low-density region.

It is also important to ask why Malin 1 has formed an apparently normal bulge, but not a normal disk. Boroson (1980) has argued that nuclear metallicity in spiral bulges is

related to bulge luminosity in the same way that nuclear luminosity is related to total luminosity in elliptical galaxies. The implication is that disk material has little influence on the processes which affect star formation in the bulge. Note that this is in contrast to the situation for S0 galaxies (Gregg 1985). Malin 1 is likely to be a striking example of a galaxy where bulge and disk formation were decoupled. The bulge presumably formed early by dissipationless collapse. However, several models allow for a slow ($\sim 10^{10}$ yr) buildup of the disk. Silk and Norman (1981) build an exponential disk by gas cloud-cloud collisions in a massive halo. Viscosity will distribute the disk mass into an exponential with scale length proportional to the time scale for star formation. This process is effective as long as the star formation rate is low, and the disk gas fraction high. Gunn (1982) has suggested that exponential disks grow by steady gas accretion from the halo, with the scale length increasing as $M_{\text{disk}}^{1/2}$. At recent epochs, the infall rate depends on the large-scale environment of the galaxy. At all epochs, the infall rate must be low enough to keep the disk stable to shear forces and therefore to keep the star formation rate low. Although the disk and bulge formations were probably decoupled, their interaction since then provides a natural mechanism for the fuelling of the active nucleus. Mass loss from the bulge will have low angular momentum and will set up the conditions for radial mass inflow when it coalesces with the gas in the disk.

b) Space Density of Massive H I Disks

Malin 1 nearly evaded detection at optical wavelengths, because the disk nebulosity was close to the limit of the Malin amplification technique. Galaxies that have not processed much of their gas into stars are more efficiently detected in the 21 cm line. Yet the small beam sizes of large radio dishes and the limited bandwidths of 21 cm receivers mean that an object like Malin 1 would evade detection for $v > 26,000$ km s⁻¹ or $v < 2000$ km s⁻¹. So what are the limits on the space density of massive H I disks? Fisher and Tully (1981) have used the off-beam measurements of their nearby galaxy survey to put upper limits on the space density of H I clouds in the mass range $10^7 < M_{\text{HI}} < 10^{10} M_{\odot}$. They also combine their work with previous upper limits to get a stronger constraint. Krumm and Brosch (1984) have put limits on more massive clouds in voids, $10^{10} < M_{\text{HI}} < 10^{11} M_{\odot}$. The overall limit on H I clouds in the range 10^7 – $10^{11} M_{\odot}$ is $< 1.3 \times 10^8 M_{\odot} \text{ Mpc}^{-3}$.

As a limit on the H I content of individual galaxies, this is not particularly severe. The space density of $M_b = -20.2$ bulges is $\sim 4 \times 10^5 \text{ Mpc}^{-3}$, so if every spiral with a luminous bulge was surrounded by a Malin 1 disk, the H I density contributed would still be a factor of 30 less than the limit. Similarly, if every Seyfert 1 nucleus with the luminosity of Malin 1 was embedded in a $10^{11} M_{\odot}$ H I disk, the combined H I density would be a factor of 250 less than the limit. Malin 1 provides evidence that our knowledge of the true galaxy population is incomplete. Optical catalogs are full of spiral galaxies with observed fractional H I contents of 5%–10%. This low fractional gas content indicates that these galaxies are well evolved and therefore exhibit relatively high surface brightness. We have argued that Malin 1 is not well evolved. By analogy, optical galaxy catalogs do not contain many examples of galaxies with fractional H I contents greater than 50%, even though such galaxies might not be rare. A probable exception to this is the DDO catalog which contains very LSB, low-mass but H I rich galaxies. These galaxies generally have angular

sizes of 3' or larger and have velocities which place them in the Local Supercluster. However, disks like that of Malin 1 are well below the surface brightness threshold for inclusion in this catalog.

Therefore, we believe that Malin 1 and its "cousins" (Table 1) are poorly represented in all existing galaxy catalogs. While it is true that there is a relation between M_{HI}/L_B and disk surface brightness for dwarfs (Hunter and Gallagher 1985), the result is influenced by selection. It is more important to determine if there is a relation between peak H I column density and disk surface brightness. The data of van der Hulst *et al.* (1987) is consistent with such a relation, as is the theoretical analysis of Shaya and Federman (1987). A class of galaxies with B(0) fainter than 25 mag arcsec⁻² and $\sigma_{\text{HI}} < 10^{19}$ cm⁻² would be missed by any survey except one using quasars as absorption probes.

The cosmological limits on the space density of massive H I clouds are as follows. The mass in H I clouds is less than 0.05% of the density required for a closed universe, $\rho_{\text{HI}} < 5 \times 10^{-4} \rho_{\text{crit}}$ (Fisher and Tully 1981). More appropriately, $\rho_{\text{HI}} < 0.006 (M_T/L_B) \rho_{\text{gal}}$, where ρ_{gal} is derived from the galaxy luminosity function of Felten (1977). As long as $M_T/L_B \leq 10$, the value used by Fisher and Tully, then H I clouds account for a negligible fraction of the mass in luminous galaxies. However, both massive cousins of Malin 1 and dwarf galaxies in the Local Group have $M_T/L_B > 10$ (Aaronson and Olszewski 1985). Given the poor constraints on M_T/L_B as a function of L_B for galaxies of all types, the cosmological contribution of galaxies with large M_T/L_B and large M_{HI} is highly uncertain. Galaxies like Malin 1 *could* contribute as much as half of the mass seen in luminous galaxies.

VI. IMPLICATIONS FOR QUASAR ABSORPTION

a) The Size of Galaxy Absorbers

Evidence is accumulating that the heavy element absorption lines seen in the spectra of high-redshift quasars originate in galaxies distributed cosmologically along the line of sight. Typical sizes derived for the absorbers are substantially larger than most galaxies observed locally. Yet direct observations of Ca II and K absorption in a galaxy close to the line of sight of a distant quasar have failed to detect absorption at projected distances beyond ~ 20 kpc from the galaxy (Bergeron 1988). Malin 1 has a significant surface density of stars and gas over a scale of ~ 200 kpc. In this section, we evaluate the impact of extreme LSB galaxies on the study of quasar absorption and look at the assumptions that go into the calculation of absorber sizes.

Apart from the choice of a cosmological model, there are several assumptions about galaxy properties that are folded into the calculation of quasar absorber sizes. The number of absorbers per unit redshift is given by $dN/dz = (cH_0)(1+z)^{1+\alpha} (1-q_0z)^{-1/2} \int_0^\infty \Phi(L)A(L)dL$, where $\Phi(L)dL = f_s \Phi_*(L/L_*)^{-s} \exp(-L/L_*) d(L/L_*)$ is the Schechter (1976) luminosity function, and $A(L/L_*) = (\pi R_*^2/2)(L/L_*)^{2t} \zeta^2$ is the cross-sectional area of the absorbers. We follow here the formalism of Wolfe *et al.* (1986). The fiducial values for the galaxy luminosity function are $\Phi_* = 1.5 \times 10^{-3}$ Mpc⁻³, $M_* = -19.5$ (corresponding to L_* for $H_0 = 100$ km s⁻¹ Mpc⁻¹), and $R_* = 11.5$ kpc (where R_* is the Holmberg radius $R_{26.5}$ for an L_* galaxy). Also, f_s is the fraction of gas-rich galaxies (Sp + Im), and $\zeta = R_{\text{HI}}/R_{26.5}$ is the ratio of H I to Holmberg sizes. The

quantity α is related to the exponent in the observed number-redshift function for quasar absorbers, $dN/dz \propto (1+z)^\alpha$ ($\alpha = \gamma - 1$ for $q_0 = 0$ and $\alpha = \gamma - 0.5$ for $q_0 = 0.5$). Values of γ range from ~ 2.3 for the Ly α clouds to ~ 1 for the damped Ly α systems. The four parameters that are the most uncertain are t , s , f_s , and ζ ; commonly adopted values are 0.4, 1.25, 0.7, and 1.5. The calculation of absorber cross sections is very sensitive to the choice of these parameters.

First, IBM have shown that the Holmberg (1975) relation, $R_{26.5} \propto L^{0.4}$, is partly a consequence of selection effects associated with sky brightness. In any selected to a limiting surface brightness, galaxies of the largest angular size will be selected at a given luminosity. If galaxy profiles are fitted by exponentials (a good assumption for Sp and dE types), then isophotal diameters will naturally scale as $L^{0.4}$. Sizes can be defined which are immune from this selection effect, such as an effective radius R_e (the radius containing half L_{tot}) or the exponential scale length α (appropriate for most dwarf galaxies). In addition, IBM have discovered a number of extremely low surface brightness galaxies, which correspond to very large values of R_e or exponential scale length at a given luminosity. Therefore the existence of *any* correlation between radius and luminosity is dubious. The second vulnerable assumption is the value of s , the slope of the faint end of the luminosity function. Kirshner *et al.* (1983) derived $s = 1.25$ for the field, but IBM demonstrated that selection effects against dwarfs of large angular size and low surface brightness lead to a large correction to the luminosity function. For example, a value of $s \sim 1.7$ is indicated in the Virgo cluster. Finally, we note some of the properties of quasar absorption line systems can be explained by populations of gas-rich dwarfs (York *et al.* 1986; Tyson 1988).

The effect of these uncertainties is illustrated in Figure 10a and 10b, where the fraction of absorber cross section coming from galaxies fainter than M is plotted against absolute magnitude M. The standard values of $s = 1.25$ and $t = 0.4$ are shown as the solid curves. The contribution of low-luminosity galaxies to the total cross section becomes greater if *either* the relation $R_e \propto L$ becomes shallower (i.e., more low surface brightness galaxies; Fig. 10a), or the luminosity function becomes steeper (i.e., more low-luminosity galaxies; Fig. 10b). In fact, for any combination of parameters such that $s - 2t \geq 1$, the integral $\int \Phi(L)A(L)dL$ diverges and faint galaxies *completely dominate the cross section*. Both of the selection effects discussed previously point to an increased contribution for faint galaxies. If the Virgo cluster values of $s = 1.7$ and $t = 0.2$ are typical of the overall galaxy population, an overwhelming fraction of the absorption path length comes from low-luminosity galaxies of low surface brightness.

There is large degree of uncertainty in our knowledge of both H I and optical sizes for normal galaxies. For example, in the calculation of the number of absorbers per unit redshift, $dN/dz \propto \zeta^2$, the ratio of H I to Holmberg diameters squared. Bosma (1981) has shown that $\zeta = 1.5$ if the R_{HI} is defined at a column density of 2×10^{20} cm⁻². Briggs and Wolfe (1989) have found that by 2.5 Holmberg radii the column density has on average dropped to below 2×10^{18} cm⁻². However, ζ is completely unknown at the column densities of *the majority* of the Mg II or C IV absorbers, $10^{15} < n_{\text{HI}} < 10^{18}$ cm⁻². It is also true that we have not uniformly measured the size distribution for galaxies in optical catalogs. Figure 11 shows the mean size of UGC galaxies as a function of velocity out to 15,000 km s⁻¹. While the mean size of an L_* spiral can be defined from this

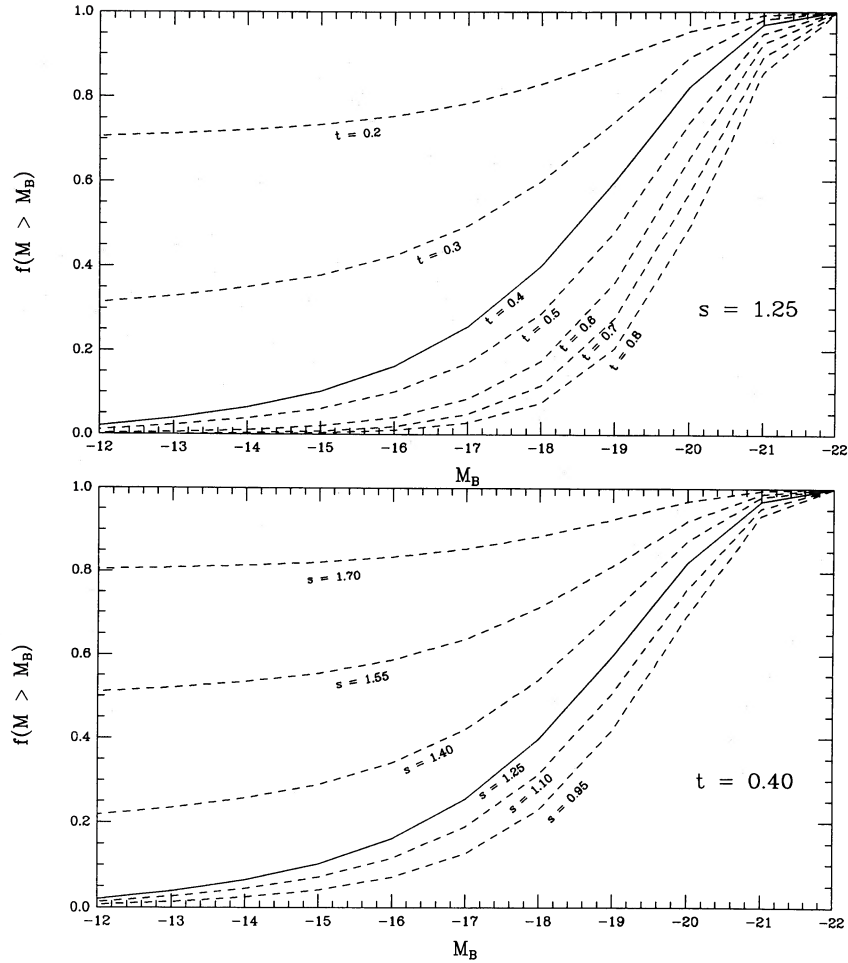


FIG. 10.—The fraction of absorption cross section contributed by galaxies fainter than M_B as a function of M_B , according to a calculation described in the text. The parameters s and t are the slope of the faint end of the galaxy luminosity function and the slope of the galaxy luminosity-radius relation. The commonly used values of $s = 1.25$ and $t = 0.4$ are plotted as solid curves.

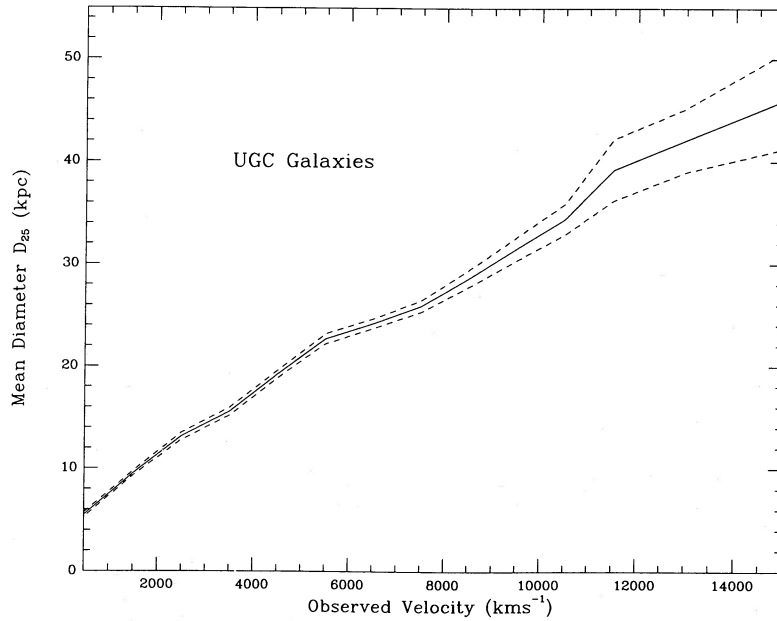


FIG. 11.—Mean diameter at the 25 mag per square arcsec isophote plotted against redshift for UGC galaxies. The dashed lines correspond to the rms error interval in diameter, for galaxies binned in velocity.

data, redshift surveys clearly do not go out far enough to sample the *tail* of the size distribution.

b) Damped Lyman- α Absorbers

Wolfe *et al.* (1986) have summarized the properties of the small class of quasar absorbers of very high H I column density ($> 10^{20} \text{ cm}^{-2}$). The disks of spiral galaxies are presumed to create the broad ($\sim 10 \text{ \AA}$), radiation damped Ly α lines seen along 20% of the lines of sight to quasars at $z \sim 2$. Could Malin 1 be a local analog of the damped Ly α systems seen at high redshift? Direct size measurements of three damped Ly α systems given lower limits of 7–8 kpc; there are no upper limits. An indirect determination of the dynamical mass of the H I absorber in front of 3C 196 is presented by Foltz, Chaffee, and Wolfe (1988). Smith *et al.* (1988) have used narrow-band imaging to put limits on Ly α emission in the absorption troughs of three systems. Assuming a Miller-Scalo IMF and a case B Ly α /H α ratio, the inferred star formation rate is less than $1 M_{\odot} \text{ yr}^{-1}$. We note that Ly α can be destroyed within a galaxy and may be an unreliable star formation indicator (Hartmann *et al.* 1988). This modest limit is consistent with the $\sim 0.1 M_{\odot} \text{ yr}^{-1}$ that the models of Talbot and Arnett (1975) predict to be produced by the extreme LSB disk of Malin 1. The properties of the two-types of gas disk are compared in columns (2) and (3) of Table 6.

A consistency check can be made on the possibility that Malin 1 type galaxies are responsible for damped Ly α absorption. The order of magnitude calculation compares dN/dz for the damped Ly α systems with the limit on dN/dz for $10^{11} M_{\odot}$ H I clouds. Wolfe *et al.* (1986) derived a range of $dN/dz = 1 - 3.5 \times 10^{-2} (H_0 = 50 \text{ km s}^{-1} \text{ Mpc}^{-1}, q_0 < 0.5, z \sim 2)$, depending on the choice of f_s and t . Our calculation gives $dN/dz = 1 - 4.5 \times 10^{-3} (H_0 = 100 \text{ km s}^{-1} \text{ Mpc}^{-1})$ at low redshift. The low value corresponds to $s - 2t = 0.45$, and the high value to $s - 2t = 0.8$ (an increased absorber contribution from faint galaxies). Using the UGC galaxies with redshifts shown in Figure 11, we get $dN/dz > 0.04$ for galaxies with $D_{25} > 50 \text{ kpc}$. This clearly demonstrates the importance for quasar absorption of the poorly sampled galaxies in the tail of the size distribution. Another uncertainty in this calculation is the value of $\zeta = R_{\text{HI}}/R_{26.5}$, as $dN/dz \propto \zeta^2$. Wolfe *et al.* (1986) used $\zeta = 1.5$ from Bosma (1981); however, Malin 1 has $\zeta = 7.5$! Taking the upper limit on $10^{11} M_{\odot}$ H I clouds of 0.02 Mpc^{-3} , the Bosma radius of Malin 1 as $\sim 200 \text{ kpc}$ and integrating over path length and inclination, the predicted number of Malin 1 absorbers per unit redshift is less than 12. Therefore, the limits on the space density of massive H I clouds at low redshift are consistent with the number of 10^{20} cm^{-2} , or greater, H I

absorbers seen at high redshift, $dN/dz \sim 0.3$. In the future, the sizes, column densities and metallicities of quasar absorbers and LSB galaxies must be compared in detail. It is a provocative thought that large and massive H I disks may have formed as early as $z \sim 2$ and remain quiescent to the present day.

VII. CONCLUSIONS

There have been observational biases against low surface brightness galaxies since the time of Messier. Our understanding to galaxy evolution will remain incomplete until we have searched hard for galaxies that have been slow to turn gas into stars. In this paper, we have argued that Malin 1 is a prototype of a quiescent disk galaxy.

1. Although Malin 1 has “cousins,” no other galaxy has the same combination of extreme low surface brightness, large size, and enormous H I mass. Malin 1 was found by accident, and the selection effects against discovering diffuse galaxies with high M_{HI}/L_B are formidable.

2. Despite its exceptional values of M_{HI} , L_B , and M_{HI}/L_B , the disk of Malin 1 has a low surface mass density of gas and an extremely low surface mass density of stars. The idea of a threshold for extensive star formation is supported by the properties of Malin 1. Among spiral galaxies, we find that high values of M_{HI}/L_B are associated with low mean H I column densities. This is a natural occurrence if the efficiency of star formation is closely linked to the surface mass density of gas, especially if the formation of massive stars depends on the intermediate step of conversion of atomic to molecular hydrogen.

3. The bulge of Malin 1 has all the absorption features of an old metal-rich stellar population, and it lies at the metal-rich end of the metallicity-luminosity relation for elliptical galaxies. The weakness of CN and the presence of weak Balmer emission give an indication of young stars near the nucleus.

4. The broad H α and strong [N II] lines are typical of a nucleus that is being photoionized by a power-law continuum. Despite the abundant fuel supply, Malin 1 lies at the faint end of the Seyfert galaxy luminosity function.

5. Malin 1 appears to be in a low-density region of the universe. This is not surprising, since such a massive H I disk would be fragile with respect to interactions. We speculate that low-density regions may be appropriate sanctuaries for diffuse galaxies with high M_{HI}/L_B . Although massive H I disks are rare, galaxies like Malin 1 could contribute as much as 50% of the mass in luminous galaxies.

6. We argue that Malin 1 is an unevolving disk galaxy. In terms of models of disk evolution, the low surface mass density of Malin 1 implies that the chemical composition and mass fraction in gas will change extremely slowly over a Hubble time. The current disk star-formation rate is predicted to be $0.1 M_{\odot} \text{ yr}^{-1}$ or less. It is likely that the disk and bulge formation processes were largely decoupled in Malin 1.

7. We have reinvestigated the assumptions that go into the calculation of galaxy cross sections for quasar absorption. When selection effects are taken into account, low-luminosity galaxies are predicted to dominate the cross section to quasar absorption.

8. The properties of Malin 1 are similar to those of the gas-rich objects responsible for damped Ly α absorption in high-redshift quasars. Larger and massive H I disks may have formed $\sim 10 \text{ Gyr}$ ago and remained unchanged to the present day.

TABLE 6
COMPARISON OF ABSORBERS

Property (1)	Malin 1 (2)	Damped Ly α Systems (3)
Size (kpc)	55	>7–8
H I column density (cm^{-2})	2×10^{20}	10^{20} – 10^{21}
Star formation rate ($M_{\odot} \text{ yr}^{-1}$)	~ 0.1	<1
dN/dz ($H_0 = 100 \text{ km s}^{-1} \text{ Mpc}^{-1}$)	$\sim 1 \times 10^{-2}$	$1 - 5 \times 10^{-3}$
Intersection Probability/Unit Redshift	<12	~ 0.3
$\rho_{\text{HI}}/\rho_{\text{crit}}(M/L = 10)$	$< 5 \times 10^{-4}$	$\sim 4 \times 10^{-4}$

We thank Dave Ouellette and the MMT staff for keeping the Blue Channel in a high state of readiness, and Andrew Alday and Janet Robertson for flawless telescope operating. Ron Maddalena provided invaluable assistance with the 140 foot observations at NRAO. We are grateful to Gary Neugebauer for obtaining the near infrared data at Palomar. John Huchra kindly allowed the use of his redshift catalog in advance of

publication. Paul Hewett made available the quasar H147 near Malin 1. We benefited from conversations with Craig Foltz, Tim Hawarden, Rob Kennicutt, Jeremy Mould, and Art Wolfe. C. D. I. received support from NSF grants INT-8600806 and AST-8700741. None of this would have been possible without the photographic wizardry of Dave Malin.

REFERENCES

- Aaronson, M. and Olszewski, E. 1985, in *IAU Symposium 177, Dark Matter in the Universe*, ed. J. Kormendy and G. R. Knapp (Dordrecht: Reidel), p. 153.
- Baldwin, J., Phillips, M., and Terlevitch, R. 1981, *Pub. A.S.P.*, **93**, 5.
- Bennett, C. L., Lawrence, C. R., Burke, B. F., Hewitt, J. N., and Mahoney, J. 1986, *Ap. J. Suppl.*, **61**, 1.
- Bergeron, J. 1988, in *QSO Absorption Lines: Probing the Universe*, ed. C. Blades, C. Norman, and D. Turnshek (Cambridge: Cambridge University Press), p. 127.
- Bergvall, N., and Jörsäter, S. 1988, *Nature*, **331**, 589.
- Bloemen, J. B. G. M., et al. 1986, *Astr. Ap.*, **154**, 25.
- Borosan, T. A. 1980, Ph.D. thesis, University of Arizona.
- Bosma, A. 1981, *A.J.*, **86**, 1825.
- Bothun, G. D. 1982, *Ap. J. Suppl.*, **50**, 39.
- Bothun, G. D., Aaronson, M. A., Schommer, R. A., Huchra, J. P., and Mould, J. R. 1984a, *Ap. J.*, **278**, 475.
- Bothun, G. D., Aaronson, M., Schommer, R., Mould, J., Huchra, J., and Sullivan, W. 1985, *Ap. J. Suppl.*, **57**, 423.
- Bothun, G. D., Heckman, T. M., Schommer, R. A., and Balick, B. 1984b, *A.J.*, **89**, 1293.
- Bothun, G. D., Impey, C. D., Malin, D. F., and Mould, J. R. 1987, *A.J.*, **94**, 23 (BIMM).
- Bothun, G. D., Romanishin, W., Margon, B., Schommer, R. A., and Chanan, G. A. 1982, *Ap. J.*, **257**, 40.
- Briggs, F. H., and Wolfe, A. M. 1989, in preparation.
- Burstein, D., Faber, S. M., Gaskell, C. M., and Krumm, N. 1984, *Ap. J.*, **287**, 586.
- Cowie, L. L., Lilly, S. J., Gardner, J., and McLean, I. S. 1988, *Ap. J. (Letters)*, **332**, L29.
- Davies, J. I., Phillips, S., and Disney, M. J. 1988, *M.N.R.A.S.*, **239**, 69P.
- Disney, M. J. 1976, *Nature*, **263**, 573.
- Elias, J. A., Frogel, J. A., Matthews, K., and Neugebauer, G. 1982, *A.J.*, **87**, 1029.
- Faber, S. M. 1977, in *The Evolution of Galaxies and Stellar Populations*, ed. B. M. Tinsley and R. B. Larson (New Haven: Yale University Press), p. 157.
- Felten, J. E. 1977, *A.J.*, **82**, 861.
- Fisher, J. R., and Tully, R. B. 1981, *Ap. J. Suppl.*, **47**, 139.
- Foltz, C. B., Chaffee, F. H., and Wolfe, A. M. 1988, *Ap. J.*, **335**, 35.
- Freedman, W. L. 1984, Ph.D. thesis, University of Toronto.
- Gallagher, J. A., and Bushouse, H. 1983, *A.J.*, **88**, 55.
- Gallagher, J. A., and Hunter, D. A. 1984, *Ann. Rev. Astr. Ap.*, **22**, 37.
- Geller, M. J., et al. 1989, *Ap. J.*, submitted.
- Goldreich, P. and Lynden-Bell, D. 1965, *M.N.R.A.S.*, **130**, 125.
- Gregg, M. D. 1985, Ph.D. thesis, Yale University.
- Gunn, J. E. 1982, in *Astrophysical Cosmology*, ed. H. A. Brück, G. V. Coyne, and M. S. Longair (Vatican: Specola Vaticana), p. 233.
- Hartmann, L. W., Huchra, J. P., Geller, M. J., O'Brien, P., and Wilson, R. 1988, *Ap. J.*, **326**, 101.
- Hawarden, T. G., Longmore, A. J., Goss, W. M., Mebold, U., and Tritton, S. B. 1981, *M.N.R.A.S.*, **196**, 175.
- Hawarden, T. G., van Woerden, H., Mebold, U., Goss, W. M., and Peterson, B. A. 1979, *Astr. Ap.*, **76**, 230.
- Haynes, M. P., and Giovanelli, R. 1984, *A.J.*, **89**, 758.
- Heckman, T. M., Sancisi, R., Sullivan, W. T., and Balick, B. 1982, *M.N.R.A.S.*, **199**, 425.
- Holmberg, E. 1975, in *Stars and Stellar Systems*, Vol. 9, *Galaxies and the Universe*, ed. A. Sandage, M. Sandage, and J. Kristian (Chicago: University of Chicago Press), p. 123.
- Huchra, J. P., and Brodie, J. 1984, *Ap. J.*, **280**, 547.
- Hunter, D. A., and Gallagher, J. A. 1985, *A.J.*, **90**, 1789.
- Impey, C. D., Bothun, G. D., and Malin, D. F. 1988, *Ap. J.*, **330**, 634 (IBM).
- Impey, C. D., Wynn-Williams, C. G., and Becklin, E. E. 1986, *Ap. J.*, **309**, 572.
- Keel, W. C. 1983, *Ap. J.*, **269**, 466.
- Kennicutt, R. C., Keel, W. C., van der Hulst, J. M., Hummel, E., and Roettiger, K. A. 1987, *A.J.*, **93**, 1011.
- Kirshner, R. P., Oemler, A., Schechter, P. L., and Schectman, S. A. 1983, *A. J.*, **88**, 1285.
- Krumm, N., and Brosch, N. 1984, *A.J.*, **89**, 1461.
- Lewis, B. M. 1987, *Ap. J. Suppl.*, **63**, 515.
- Lilly, S. J. 1988, *Ap. J.*, **333**, 161.
- Longmore, A. J., Hawarden, T. G., Cannon, R. D., Allen, D. A., Mebold, U., Goss, W. M., and Reif, K. 1979, *M.N.R.A.S.*, **188**, 285.
- Malin, D. F. 1978, *Nature*, **276**, 591.
- McCarthy, P. J., Spinrad, H., Djorgovski, S., Strauss, M. A., van Breugel, W., and Leibert, J. 1987, *Ap. J. (Letters)*, **319**, L9.
- Meurs, E. J. A., and Wilson, A. S. 1984, *Astr. Ap.*, **136**, 206.
- Osterbrock, D. E. 1977, *Ap. J.*, **215**, 738.
- Quirk, W. J. 1972, *Ap. J. (Letters)*, **176**, L9.
- Romanishin, W., Krumm, N., Salpeter, E., Knapp, G., Strom, K. M., and Strom, S. E. 1982, *Ap. J.*, **263**, 94.
- Schechter, P. A. 1976, *Ap. J.*, **203**, 297.
- Schmidt, M. 1959, *Ap. J.*, **129**, 243.
- Schommer, J. A., and Bothun, G. D. 1983, *A.J.*, **88**, 577.
- Shaya, E. J., and Federman, S. R. 1987, *Ap. J.*, **319**, 76.
- Silk, J., and Norman, C. A. 1981, *Ap. J.*, **247**, 59.
- Smith, H. E., Cohen, R. D., and Burns, J. E. 1988, in *QSO Absorption Lines: Probing the Universe*, ed. C. Blades, C. Norman, and D. Turnshek (Baltimore: Space Telescope Science Institute), p. 148.
- Spinrad, H., Fillipenko, A. V., Wyckoff, S., Stocke, J. T., Wagner, R. M., and Lawrie, D. G. 1985, *Ap. J. (Letters)*, **299**, L7.
- Talbot, R. J., and Arnett, W. D. 1975, *Ap. J.*, **197**, 551.
- Tonry, J. T., and Davis, M. A. 1979, *A.J.*, **84**, 1511.
- Tully, R. B., and Fisher, J. R. 1977, *Astr. Ap.*, **54**, 661.
- Tyson, N. D. 1988, *Ap. J. (Letters)*, **329**, L57.
- van der Hulst, J. M., Skillman, E. D., Kennicutt, R. C., and Bothun, G. D. 1987, *Astr. Ap.*, **177**, 63.
- Warmels, R. H. 1988a, *Astr. Ap. Suppl.*, **72**, 19.
- . 1988b, *Astr. Ap. Suppl.*, **72**, 57.
- . 1988c, *Astr. Ap. Suppl.*, **72**, 427.
- Williams, T. B. 1976, *Ap. J.*, **209**, 716.
- Wolfe, A. M., Turnshek, D. A., Smith, H. E., and Cohen, R. D. 1986, *Ap. J. Suppl.*, **61**, 249.
- York, D. G., Dopita, M., Green, R., and Bechtold, J. 1986, *Ap. J.*, **311**, 610.
- Young, J. S., and Scoville, N. Z. 1982, *Ap. J.*, **268**, 467.
- Young, P. J., Westphal, J. A., Kristian, J., Wilson, C. P., and Landauer, F. P. 1978, *Ap. J.*, **211**, 721.

GREG BOTHUN: Astronomy Department, Dennison Building, University of Michigan, Ann Arbor, MI 48109

CHRIS IMPEY: Steward Observatory, University of Arizona, Tucson, AZ 85721